Point 2 Selectrons and the Standard Model Background

Nick Danielson and Liz Goodman
University of Colorado

August 31, 1998

1 Introduction

One of the leading theories of particle physics beyond the Standard Model is Supersymmetry [1]. By examining Monte Carlo simulations of e^+e^- collisions, we hope to develop techniques for discovering Supersymmetry and for determining the masses of the various supersymmetric particles. Since there are many possible versions of Supersymmetry theory, theorists have given us five points in parameter space designed to encompass most of the range of supersymmetric phenomena based on the minimal SUGRA model with R-parity conservation [2]. For instance, Table 1 shows the masses of various supersymmetric particles in each of the five different points. This paper focuses on 500 GeV point 2 selectron ($\widetilde{e}^{\pm}$) production and methods for separating this signal from the Standard Model backgrounds shown in Table 2. A series of cuts is discussed which greatly reduces these backgrounds while leaving the selectron signal almost unchanged.

2 The selectron signal

Table 3 shows the cross sections of supersymmetric modes from e^+e^- annihilation at 500 GeV and 80% and 60% right and 80% and 60% left polarizations[1]. The supersymmetric data was generated with ISAJET [3]. In this

[1]In order to avoid *any possible confusion*, 80% left polarization is EPOL=0.8

Table 1: Particle masses for points 1–5. This data was generated with ISAJET [3].

	Point 1	Point 2	Point 3	Point 4	Point 5
$\widetilde{\chi}_1^0$	86.05	128.70	44.52	77.83	57.17
$\widetilde{\chi}_2^0$	175.45	257.22	97.00	115.29	111.46
$\widetilde{\chi}_3^0$	492.70	535.50	256.94	146.84	444.77
$\widetilde{\chi}_4^0$	501.75	542.54	273.64	292.41	464.60
$\widetilde{\chi}_1^\pm$	175.34	257.20	96.39	96.06	110.10
$\widetilde{\chi}_2^\pm$	500.81	542.24	272.04	292.46	461.60
h^0	83.25	89.92	68.29	126.96	101.42
H^0	745.30	681.40	378.99	201.61	622.61
A^0	741.05	676.41	371.09	200.00	620.01
$H^\pm$	744.61	680.33	378.49	214.81	624.10
$\widetilde{\nu}_L$	421.40	230.02	206.62	1000.00	314.60
$\widetilde{e}_L^\pm$	425.92	238.21	215.70	1000.00	320.64
$\widetilde{e}_R^\pm$	408.80	156.95	206.54	1000.00	307.45
$\widetilde{t}_1$	424.43	535.82	263.71	924.84	150.66
$\widetilde{b}_L$	520.57	621.86	274.27	1000.00	380.76
$\widetilde{q}_L$	603.27	668.38	316.73	1000.00	462.49
$\widetilde{t}_2$	550.61	656.48	329.48	1096.29	494.73
$\widetilde{b}_R$	595.55	653.10	312.97	1000.00	456.58
$\widetilde{q}_R$	603.27	668.38	316.73	1000.00	462.49
$\widetilde{g}$	550.62	759.04	298.40	900.00	425.52

paper, we are interested in the selectron production mode ($e^+e^- \to \widetilde{e}^+\widetilde{e}^-$). There are two selectrons — one left-handed and one right-handed — each with a different mass as shown in Table 1. Thus there are four different selectron production modes: $\widetilde{e}_L^+\widetilde{e}_L^-$, $\widetilde{e}_L^+\widetilde{e}_R^-$, $\widetilde{e}_R^+\widetilde{e}_L^-$, and $\widetilde{e}_R^+\widetilde{e}_R^-$. The cross sections for these processes change depending on the beam polarization, as Table 3 reveals. We simulated 500 GeV 80% and 60% right and 80% and 60% left polarized data. We will discuss the results of the 80% polarized signal first, and then we will discuss the 60% polarized case in a later section. The selectron always decays into an electron and a neutralino ($\widetilde{\chi}_1^0$). The neutralino escapes undetected, so the selectron signal is exactly two particles: one electron and one positron, and missing energy.

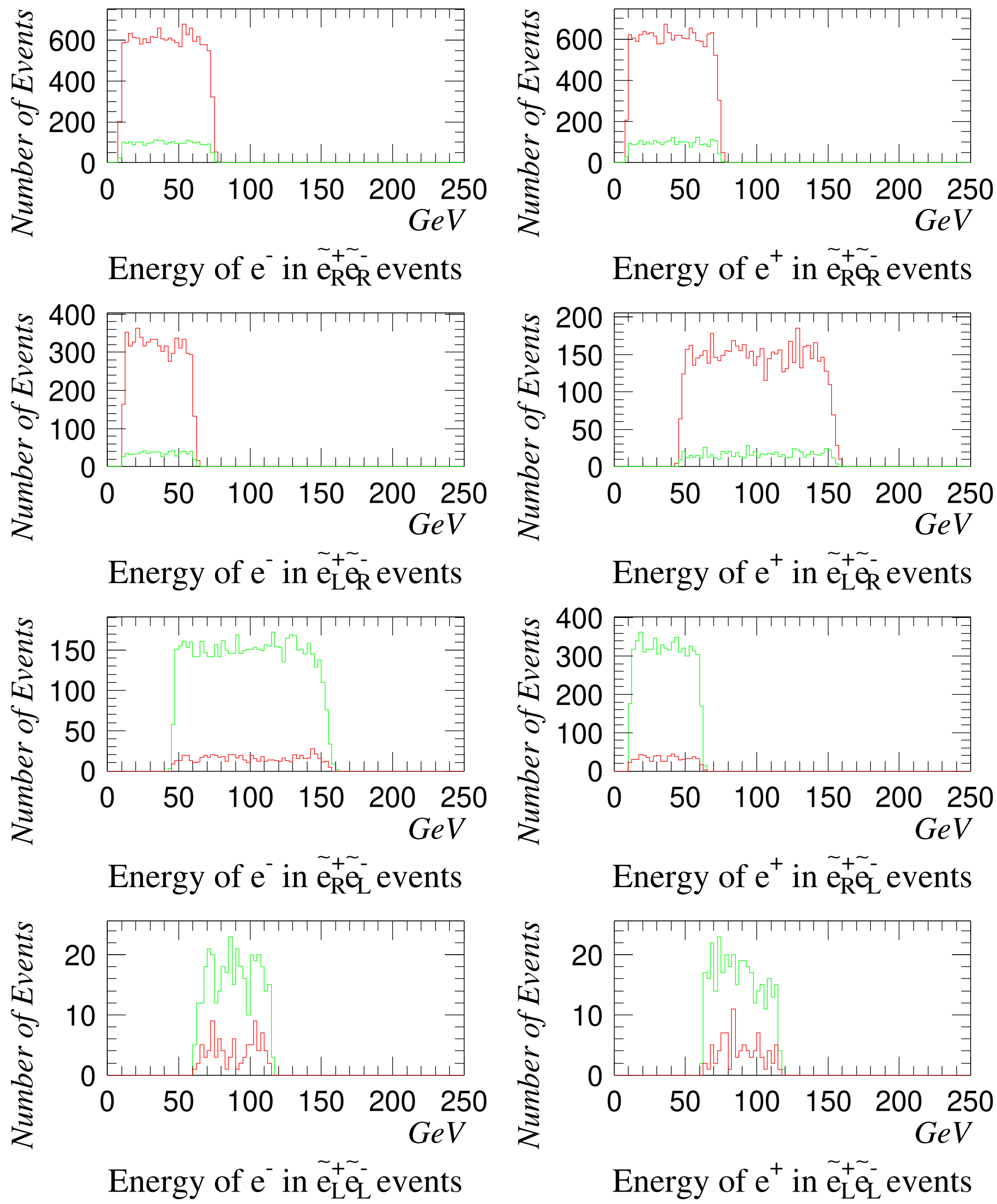

Figure 1: The energy distribution of electrons and positrons that come from the various selectron production modes. The 80% right polarized data is red, the 80% left polarized data is green. This data represents 50 fb^{-1} of data.

Table 2: Cross sections (in fb) for Standard Model processes at 500 GeV.

Mode	Cross section (fb)			
$\gamma^*\gamma^*$	4.42×10^7			
$\gamma\gamma$	6840			
γ^* or Z^0	5380			
$\gamma\gamma^*$ or Z^0	5200			
Z^0Z^0	427			
	80% Left	60% Left	60% Right	80% Right
W^+W^-	12710	11300	2866	1461

Table 3: Cross sections (in fb) for various point 2 production modes. In this table, $\widetilde{\ell} = \widetilde{\mu} + \widetilde{\tau}$. This data was generated with ISAJET [3].

	500 GeV			
	80% Left	60% Left	60% Right	80% Right
$\widetilde{\chi}^0_1\widetilde{\chi}^0_1$	65	107	364	404
$\widetilde{\chi}^0_1\widetilde{\chi}^0_2$	63	56	14	7
h^0Z^0	70	69	57	54
$\widetilde{\nu}_e\overline{\widetilde{\nu}}_e$	121	109	29	16
$\widetilde{e}^+_L\widetilde{e}^-_L$	7	6	2	2
$\widetilde{e}^+_R\widetilde{e}^-_R$	53	86	283	317
$\widetilde{e}^\pm_L\widetilde{e}^\mp_R$	145	143	145	146
$\widetilde{\ell}^+_R\widetilde{\ell}^-_R$	25	31	68	75
$\widetilde{\ell}^+_L\widetilde{\ell}^-_L$	50	63	137	150
Total	590	655	1040	1104

Selectron decays are of two types:

1. $e^+e^- \rightarrow A + \bar{A}$ (where $\mathrm{m}_A = m_{\bar{A}}$, for instance $e^+e^- \rightarrow \widetilde{e}^+_L\widetilde{e}^-_L$ and $e^+e^- \rightarrow \widetilde{e}^+_R\widetilde{e}^-_R$)

2. $e^+e^- \rightarrow A + B$ (where $\mathrm{m}_A \neq m_B$, for instance $e^+e^- \rightarrow \widetilde{e}^+_L\widetilde{e}^-_R$).

In both types, $A \rightarrow C + D$ ($\widetilde{e}^\pm \rightarrow \widetilde{\chi}^0_1 + e^\pm$), and the energy distribution of D is a box whose endpoints depend on the mass of C. By measuring the

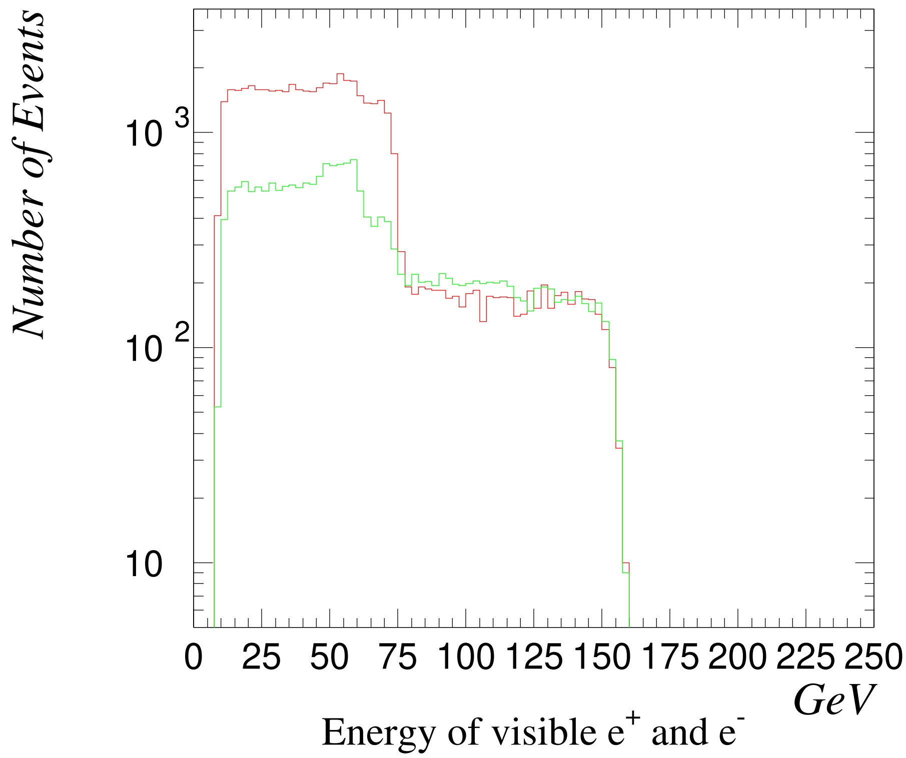

Figure 2: The energy distribution of electrons and positrons that come from selectron events. This is the sum of all the plots in Figure 1. The 80% right polarized data is red while the 80% left polarized data is green. This data represents 50 fb^{-1} of data.

endpoints of D's energy distribution, the mass of C can be calculated [4], [5], [6]. Consider, for instance, an $e^+e^- \rightarrow \widetilde{e}_L^+\widetilde{e}_R^-$ event. The $\widetilde{e}_R^-$ decays into an e^-, while the $\widetilde{e}_L^+$ decays into an e^+ to preserve charge. Since the masses of the $\widetilde{e}_L$ and $\widetilde{e}_R$ are different, the energy distribution of the $e^-$and e^+ will be different. Figure 1 shows the energy distributions of electrons and positrons that come from each of the four different selectron production modes. Figure 2 is the sum of these plots. This sum is the selectron signal that must be separated from our Standard Model background. This signal is important because the relative sizes of the two main boxes change with beam polarization, and there is no similar Standard Model signal whose height depends on beam polarization in this manner.

3 The Standard Model background

In a real detector, the selectron signal is mixed with various backgrounds. Our background includes the particles that are expected to exist according to the Standard Model, in quantities that have been predicted by theorists. Table 2 lists the cross sections in fb for our Standard Model background production modes at 500 GeV.

3.1 The $\gamma^*\gamma^*$ background

The background with the largest cross section is the $\gamma^*\gamma^*$ process. Our $\gamma^*\gamma^*$ data was generated with the Monte Carlo simulator HERWIG [7].

The $\gamma^*\gamma^*$ intermediate state leads to the production channels shown in Table 4. The $\gamma^*\gamma^*$ production modes other than the e^+e^- mode do not

Table 4: Production modes for $\gamma^*\gamma^*$.

Mode	Cross section (fb)	Fraction
e^+e^-	2.76×10^7	62.35%
$\mu^+\mu^-$	1.24×10^7	28.07%
hadrons	3.93×10^6	8.88%
$\tau^+\tau^-$	3.09×10^5	0.70%
W^+W^-	111	0.02%

present a serious background problem for selectron events. Figure 3 shows the Feynman diagram for the first process shown in Table 4 ($e^+e^- \to \gamma^*\gamma^*e^+e^- \to e^+e^-e^+e^-$). In this process there are four final particles: two electrons and two positrons. One electron and one positron are produced by the virtual photons; they are generally visible with very low energy. The other electron and positron are the slightly deflected initial state particles. They tend to have very high energy (just under 250 GeV) and they almost always go down the beamhole (inside 100 mrad).

These $\gamma^*\gamma^*$ events look very similar to selectron events because there are exactly two visible particles — an e^- and an e^+ — and a great deal of missing energy. As mentioned above, the $\gamma^*\gamma^*$ events are particularly adverse for the search for Supersymmetry because their cross section is very high compared to supersymmetric cross sections. At 500 GeV the cross section for $e^+e^- \to \gamma^*\gamma^*e^+e^- \to e^+e^-e^+e^-$ is 2.76×10^7 fb, while the selectron production cross section is 465 fb for 80% right longitudinal e^- polarization.

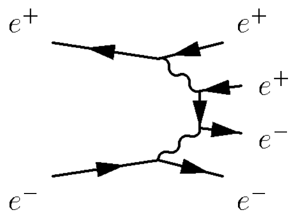

Figure 3: The production of lowest order $\gamma^*\gamma^*$ events.

3.1.1 Higher order $\gamma^*\gamma^*$ processes

Figure 4 shows next to lowest order two photon processes. It is expected that these (and higher-order processes) will increase the cross section for $e^+e^- \to e^+e^-e^+e^-$ events. The cross section that HERWIG uses is always just the lowest order. $\gamma^*\gamma^*$ interactions are of special importance in areas of moderate to small p_t, which is where the visible decay products of selectron processes appear.

3.2 The $\gamma\gamma$ process

The γ is massless, stable, and is detected in the calorimeter. It is therefore simple to eliminate this background.

3.3 The Z^0 processes

The Z^0 decay modes are shown in Table 5. The hadrons, $e^\pm$, and $\mu^\pm$ are almost always observed, the neutrinos are unobserved, and the τs decay. Missing energy results from the neutrinos and any particles that are unobserved due to detector inefficiency.

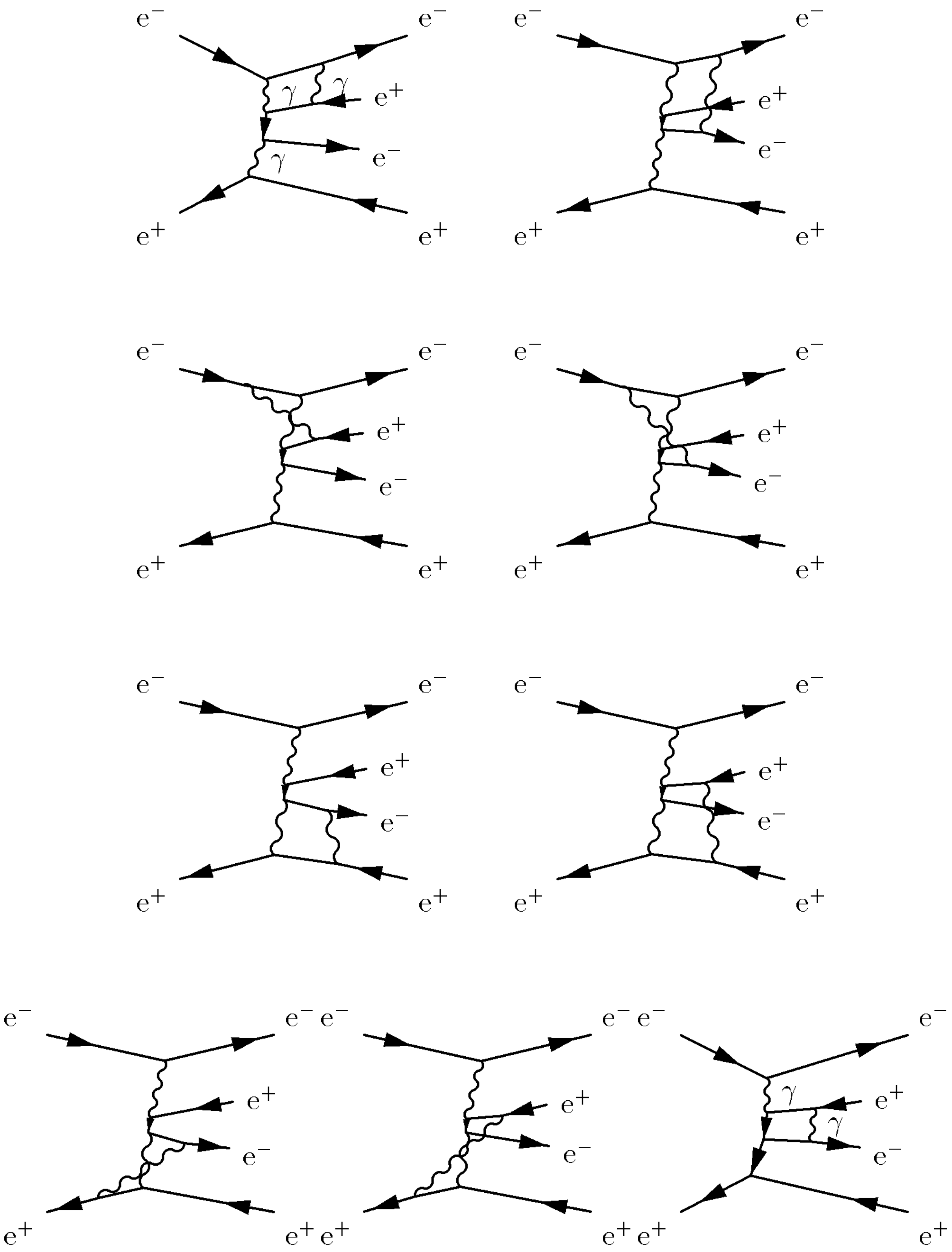

Figure 4: Next-to-lowest-order $\gamma^*\gamma^*$ processes.

Table 5: Decay modes for Z^0.

Mode	Fraction
hadrons	69.90%
neutrinos	20.01%
e^+e^-	3.37%
$\mu^+\mu^-$	3.37%
$\tau^+\tau^-$	3.37%

3.4 $\mathbf{W^\pm}$ processes

The W particle decay modes are shown in Table 6. The cross section for the W^+W^- is highly dependent on polarization because the production can occur two ways (as shown in Figure 5). In the first case, a neutrino is exchanged. Since there are no right-handed neutrinos, this process only occurs for left-handed polarizations and the cross section for left-handed W^+W^- is much higher than the right-handed cross section. The other W boson production process involves the exchange of a Z^0 or a photon, and can occur for either left- or right-handed polarizations.

Table 6: Decay modes for W^+.

Mode	Fraction
hadrons	67.8%
$e^\pm\nu(\bar{\nu})$	10.8%
$\mu^\pm\nu(\bar{\nu})$	10.6%
$\tau^\pm\nu(\bar{\nu})$	10.8%

When the Ws decay into hadrons, little or no energy is lost and the visible energy for the event is approximately 500 GeV. When the Ws decay into leptons and neutrinos, the neutrinos always leave undetected. All $W^\pm \to \ell^\pm$ decays involve the loss of energy due to neutrinos.

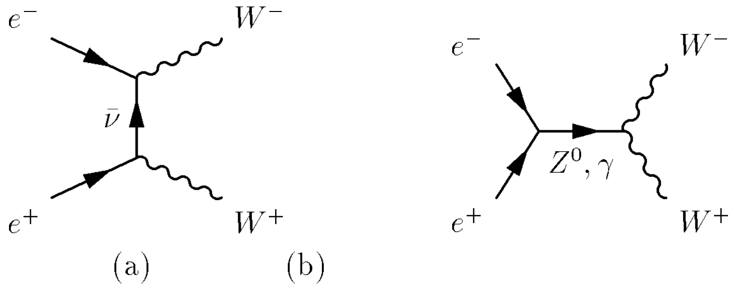

Figure 5: The two paths for W^+W^- production.

4 Cuts for removing Standard Model backgrounds other than $\gamma^*\gamma^*$

Cut 1 Figure 6 shows the energy of each electron or positron for the Standard Model backgrounds (blue) listed in Table 2 and Supersymmetric signal (red) at 500 GeV, 80% right polarization, after limiting the events to those with exactly two visible particles: one electron and one positron. This dramatically reduces the background.

In Z^0 Z^0 processes, only two types of events pass this first cut. The first is when both Z^0 decay into $e^\pm$, with one e^+ and one e^- going down the beamhole. The probability of producing four leptons is .11%, and the probability of one electron and one positron going down the beamhole is even lower. The second way is if one Z^0 decays into e^- + e^+ and the other Z^0 decays into neutrinos (thus producing exactly two visible particles). The probability of $Z^0 Z^0 \to e^- + e^+ + \nu + \bar{\nu}$ is 0.6%, so this drastically reduces the number of Z^0 Z^0 events.

The probability of *both* W particles decaying into $e^\pm\nu(\bar{\nu})$ is $10.8\% \times 10.8\% = 1.17\%$.

All selectron events result in the production of an electron and a positron. Therefore, this cut only affects the supersymmetric signal when the electron or the positron goes down the beampipe.

The Supersymmetric signal is now distinguishable from that of the background. In order to make our mass measurements, we need additional cuts to observe the leading and lagging edges of the electron or positron energy distribution.

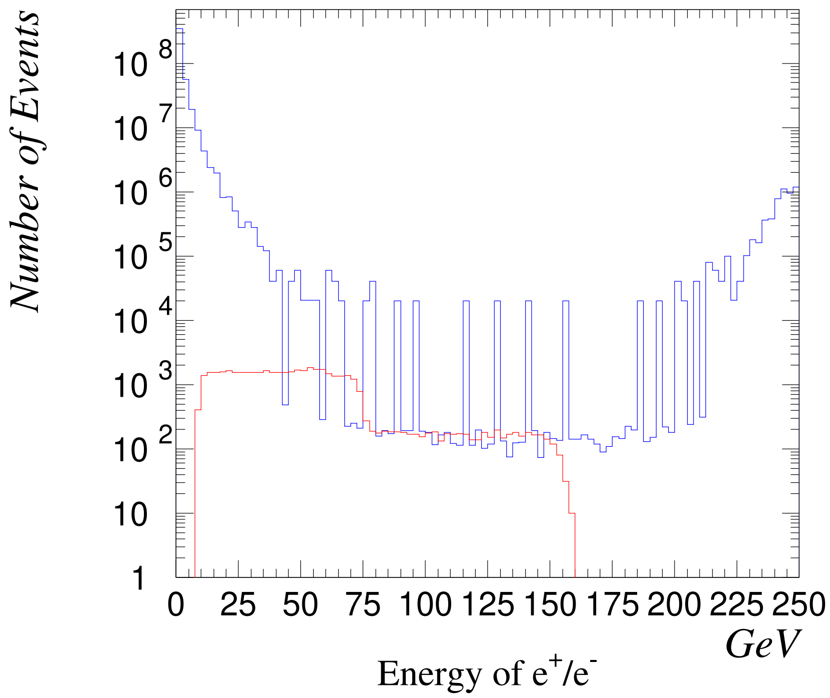

Figure 6: E_{e^+,e^-} for Supersymmetric signal (red) and Standard Model background (blue) following cut to limit events to those with exactly two visible particles: one electron and one positron. E_{cm} = 500 GeV, 80% right polarization.

Cut 2 In Standard Model events, the $e^+ + e^- \rightarrow W^+ + W^-$ occurs either with the exchange of a Z^0 or γ particle or with the exchange of a ν. In the first case, the cross section is approximately proportional to $1 + \cos^2(\theta)$ (θ is measured relative to the beam axis); with the exchange of a ν, the cross section is proportional to $1/\sin^4\frac{\theta}{2}$. In both cases, the resulting cross section is much bigger for θ near 0 and π. The selectron events do not exchange the ν or the Z^0, and decay products are approximately uniform through all angles. Figure 7 shows the angular distribution of particles in the detector. Varying the polarization does not affect the shape of angular distribution. electrons enhance the neutrino exchange process, but the decay products are still peaked near θ near 0 and π.

The second cut, Figure 8, limits the events to those that have less than

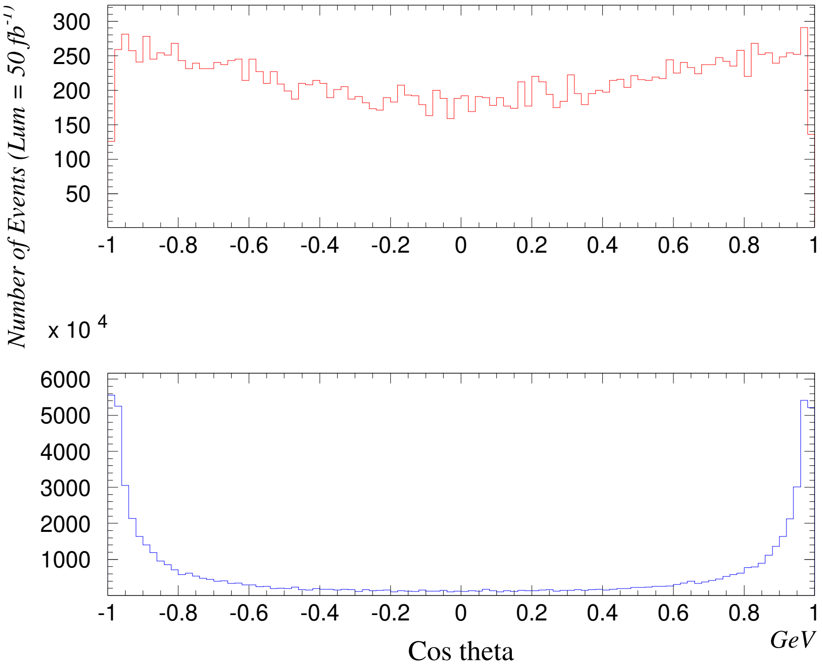

Figure 7: Cos(θ) for visible particles at 500 GeV, 60% right polarization. The spectrum for Supersymmetric particles (top, red) is approximately uniform through all angles. The spectrum for Standard Model background particles (bottom, blue) peaks at cos(θ) near $\pm$ 1.

1 GeV visible energy between $.90 < \mid \cos(\theta) \mid < .995$.[2] Figure 7 shows that the e^+ or e^- from selectrons occur approximately uniformly through all angles and that background particles occur mostly along the beam axis toward $|\cos(\theta)| = 1$. By removing events with energy between $.90 < |\cos(\theta)| < .995$, we reduce the Standard Model background without much affecting the Supersymmetric signal.

Cut 3 If there were no invisible particles leaving the detector, and if the detector was perfectly efficient, the energy in the forward direction[3] should be $\sim 1/2$ E_{cm}, and the energy in the backward direction should be $\sim 1/2$ E_{cm}.

[2] We use $\pm .995$ for our upper limit because energy is not visible above $|cos(\theta)| = 0.995$.

[3] The forward direction is the hemisphere around the thrust axis that has more visible energy.

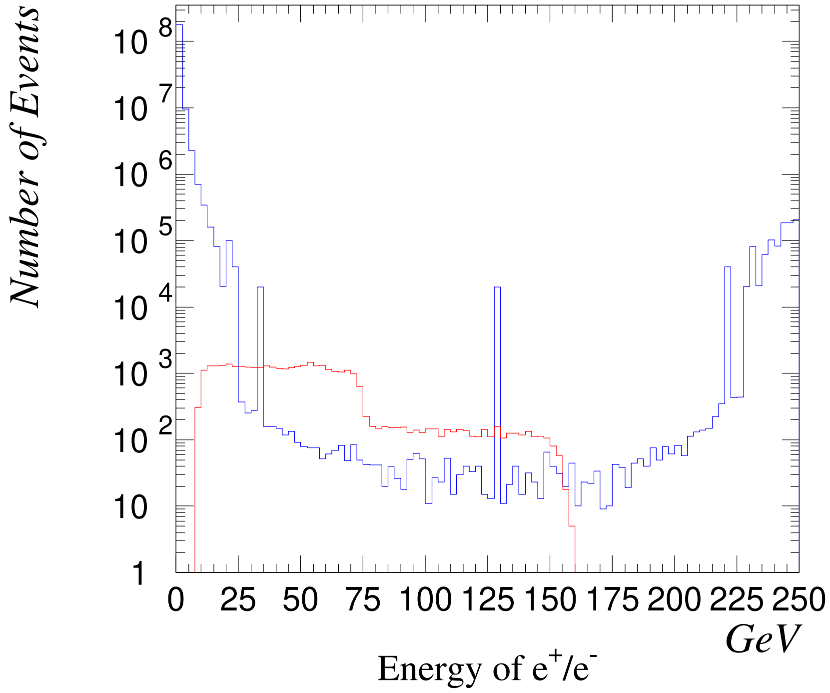

Figure 8: E_{e^+,e^-} for Supersymmetric signal and Standard Model background following cut to limit events to those with less than 1 GeV visible energy between 0.9< $|\cos(\theta)|$ <.995. E_{cm} = 500 GeV, 80% right polarization.

Nevertheless, all Supersymmetric events have some energy missing (usually in both hemispheres), and therefore will not have $E_{forward} \sim 1/2$ E_{cm}. Figure 9 only includes events with visible energy in the forward direction less than 1/2 E_{cm} minus 10% E_{cm}.[4]

The Supersymmetric events generally produce an electron and a neutralino in one hemisphere, and a positron and a neutralino in the other hemisphere. Neither hemisphere has energy greater than 1/2 E_{cm} minus 10% E_{cm}. Therefore, by cutting out events with energy greater than 1/2 E_{cm} minus 10% E_{cm}, we remove background without affecting the signal.

This set of cuts is the most effective way we found of reducing the non-$\gamma^*\gamma^*$ background without changing the endpoints of the visible energy histogram for the signal. To summarize, the cuts we used are:

[4]The 10% is subtracted to account for detector inefficiency and resolution.

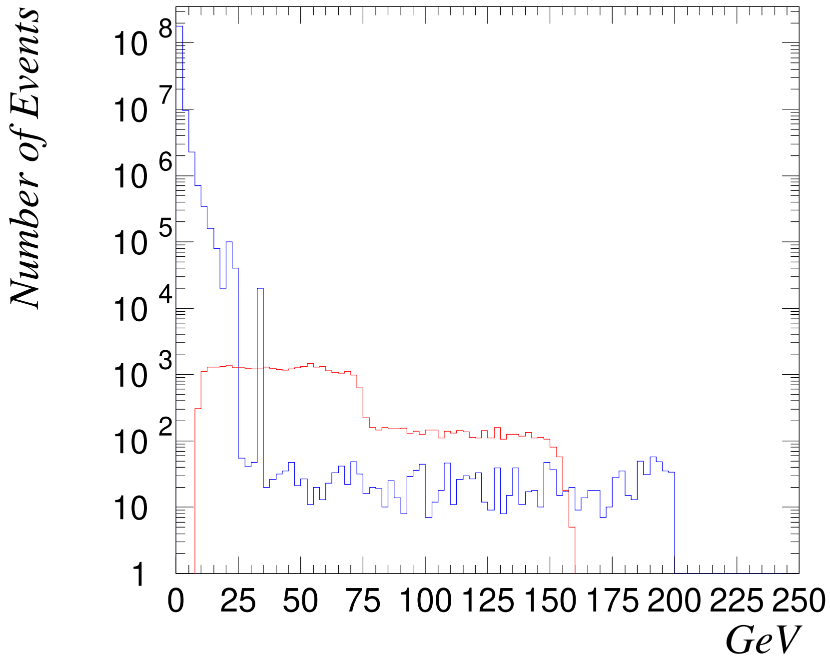

Figure 9: E_{e^+,e^-} for Supersymmetric signal (red) and Standard Model background (blue) following cut to limit events to those with energy in the forward direction less than 0.4 E_{cm}. E_{cm} = 500 GeV, 80% right polarization.

1. All events must have exactly two visible particles: one e^+ and one e^-.
2. All events must have less than 1 GeV visible energy between $.90 < |\cos(\theta)| < .995$.
3. Limit events to those with energy in the forward direction less than 0.4 E_{cm}.

We will refer to these three cuts as the "standard" cuts from now on.

5 Cuts for removing the $\gamma^*\gamma^*$ background

In order to separate selectron events from the $\gamma^*\gamma^*$ background, a cut on the event's total transverse momentum (p_t) can be made in addition to the previous standard cuts. The event's total transverse momentum is defined as:

$$p_t^2 = (\sum_i p_{x,i})^2 + (\sum_i p_{y,i})^2$$

where i runs over all the visible particles in the event. In this case there are only two visible particles: an electron and a positron.

Figure 10 shows the total p_t for selectron events and for two photon events. Notice that the $\gamma^*\gamma^*$ events' p_t is lower than the selectron events', and is quite steep.

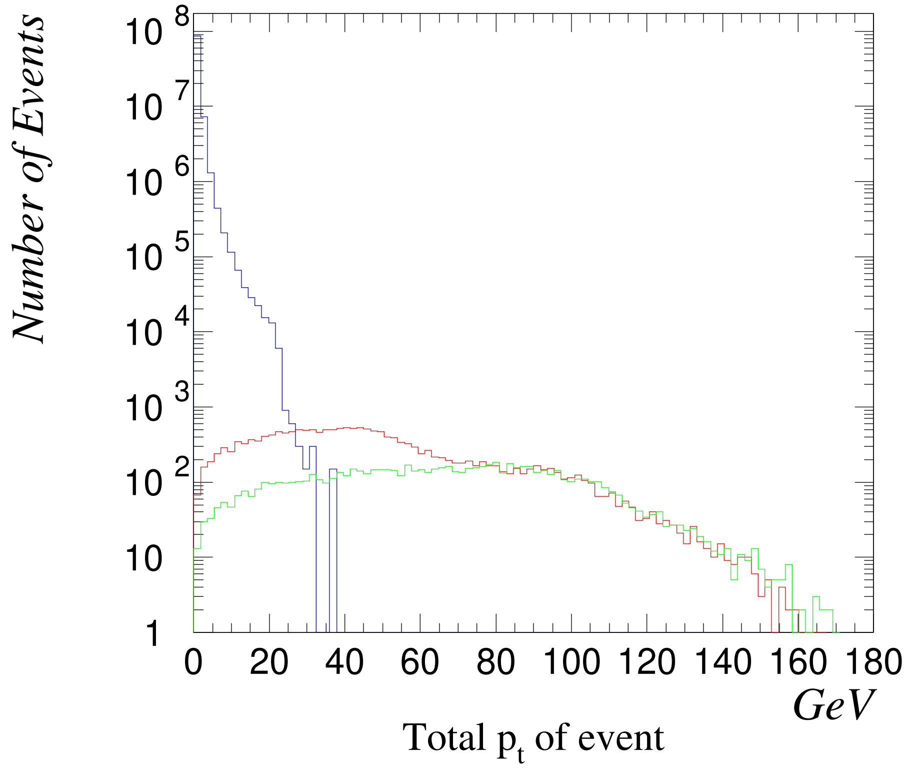

Figure 10: The total transverse momentum of $\gamma^*\gamma^*$ events (blue) and selectron events (red for 80% right polarized data, green for 80% left polarized data). This represents 50 fb^{-1} of data.

Figure 11 shows the energy distribution of electrons and positrons in both selectron and $\gamma^*\gamma^*$ events as the p_t cut is varied. When the total p_t cut is set at 40 GeV/c, most of the $\gamma^*\gamma^*$ background is removed. This cut also removes those selectron events where the electron/positron energy is low.

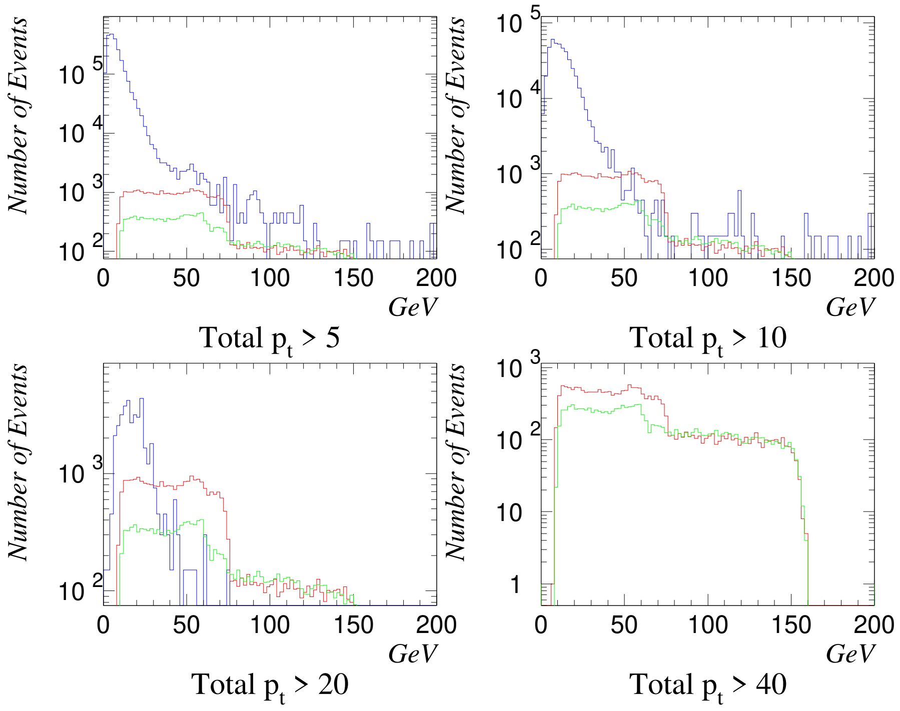

Figure 11: The energy of electrons and positrons as the cut on total transverse momentum is varied. The 80% right polarized selectron data is red, the 80% left polarized data is green, and the $\gamma^*\gamma^*$ data is blue. This represents 50 fb^{-1} of data.

Figure 12 shows all the Standard Model backgrounds along with the selectron signal when the three standard cuts are made in addition to a p_t cut of 40 GeV/c. The selectron signal's energy endpoints remain virtually unchanged, but the relative heights of the two boxes *have* changed. Thus the mass measurement can be accomplished with this cut, but a measurement of the relative cross sections of the various selectron production modes is compromised. However, when the total p_t cut is around 10–20 GeV/c, the relative heights of the selectron signal remain almost unaffected, although the overall height of the signal has been reduced. The remaining background can be removed if our detector can see the higher energy electron/positron at an angle larger than 40 mrad.

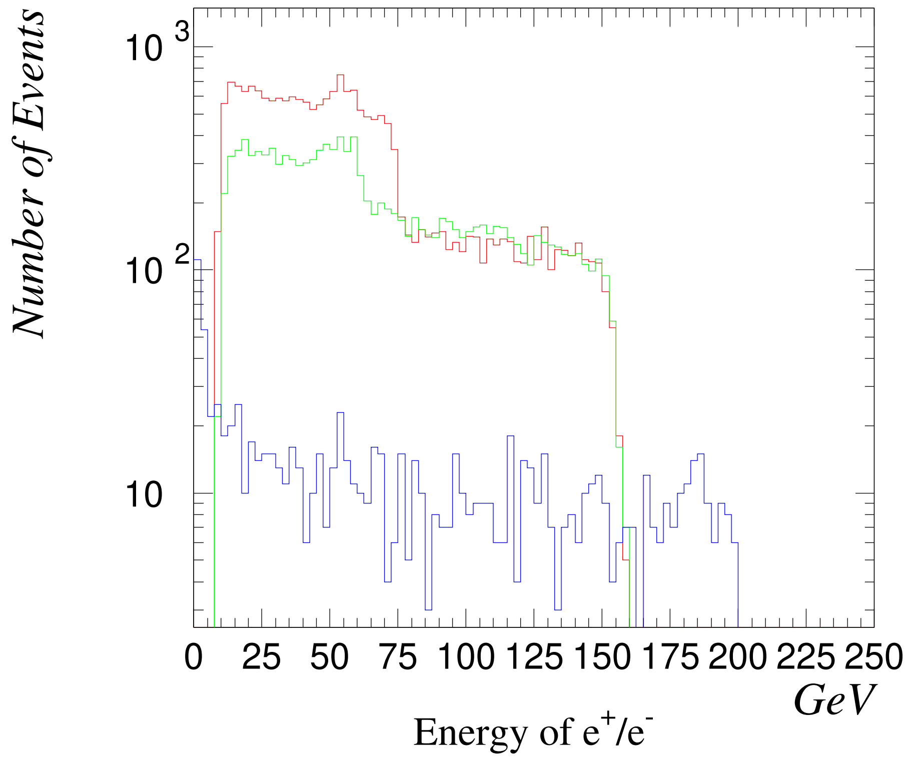

Figure 12: The energy of electrons and positrons in Standard Model (blue) and selectron events (red for 80% right, green for 80% left) with the three standard cuts and a p_t cut of 40 GeV/c.

As mentioned above, $\gamma^*\gamma^*$ events typically have two high energy particles (one electron and one positron) that go down the beam pipe and are therefore invisible to our detector. It is interesting to look at the particle with the highest angle relative to the beam axis because this one would be the easiest to detect if we had a detector that could see down to angles smaller than 100 mrad. Figure 13 shows a histogram of this particle's angle as we vary the p_t cut. Almost all the background can be eliminated if our detector can see down to 40 mrad and if we make a p_t cut of 15 GeV/c. Figure 14 shows the energy distribution of all visible electrons and positrons in both selectron and Standard Model events after all five cuts are applied:

- The three standard cuts described above
- The total p_t must be greater than 15 GeV/c
- Cut events with electrons with an angle between 40 mrad and 100 mrad. This cut amounts to assuming that the detector can see down to 40 mrad.

Most of the background is removed with these cuts, and the signal's endpoints and relative heights remain almost unaffected.

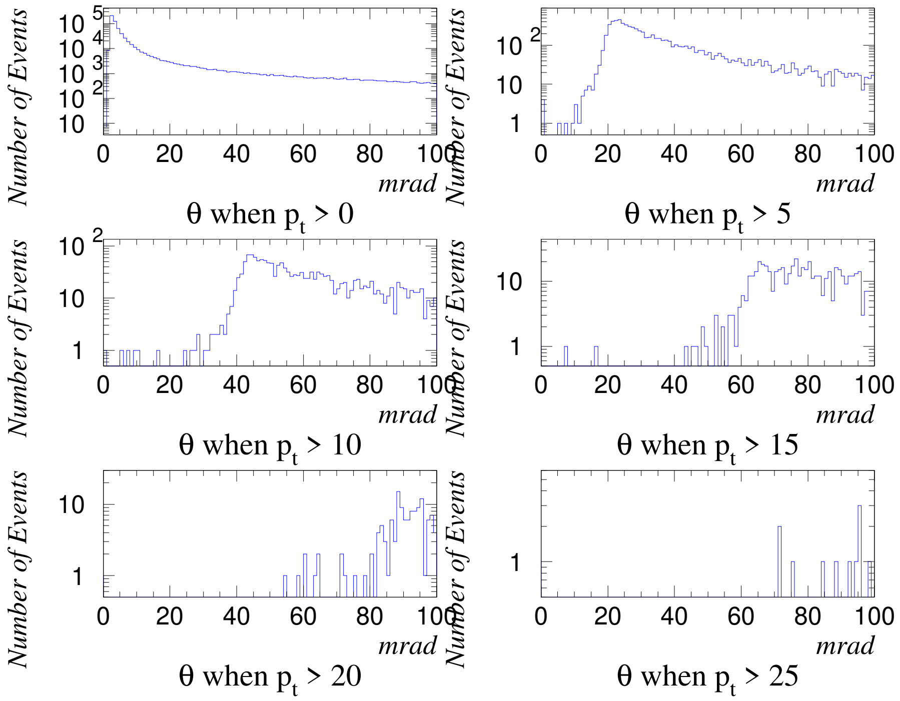

Figure 13: The angle (in mrad) of the particle with the largest angle that went down the beam pipe. Each plot corresponds to a different p_t cut. This represents only .33 fb^{-1} of two photon data.

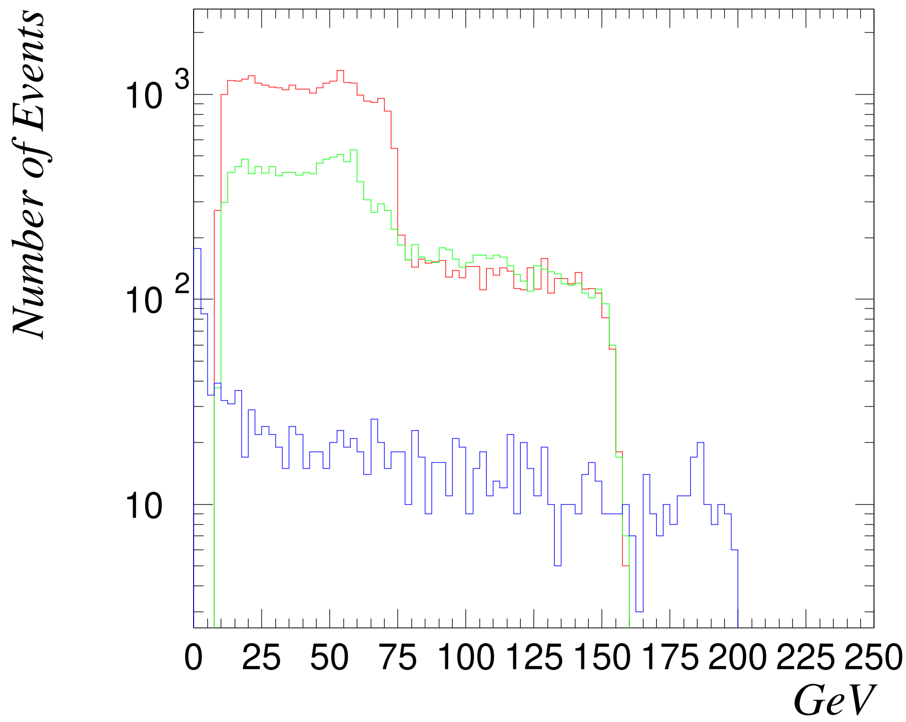

Figure 14: The energy of electrons and positrons after the five cuts described in the paper. Red is 80% right polarized selectron events, green is 80% left polarized selectron events, and blue is Standard Model events. This represents 50 fb^{-1} of data.

6 Mass Calculation

We use the endpoints of the box fit to the $\tilde{e}_R^{\pm}\tilde{e}_R^{\mp}$ signal as the values of E_{minrr} and E_{maxrr}.

$$
\begin{aligned}
m_{\tilde{\ell}_R}^2 &= E_{cm}^2 \left[\frac{E_{maxrr} E_{minrr}}{(E_{maxrr} + E_{minrr})^2} \right] \\
m_{\tilde{\chi}_1^0}^2 &= E_{cm}^2 \left[\frac{E_{maxrr} E_{minrr}}{(E_{maxrr} + E_{minrr})^2} \right] - 2E_{cm} \frac{E_{maxrr} E_{minrr}}{E_{maxrr} + E_{minrr}}
\end{aligned}
$$

Once we know the masses of the $\widetilde{\ell}_R$ and the $\widetilde{\chi}_1^0$, we use them with E$_{maxrl}$ from the histogram of the energy of all electrons and positrons to find the mass of the $\widetilde{\ell}_L$.

$$\begin{aligned}
&m^4_{\widetilde{\ell}_L} \quad (E_{cm} - 2E_{maxrl}) + \\
&m^2_{\widetilde{\ell}_L} \quad (4E_{cm}E^2_{maxrl} - 2E^2_{cm}E_{maxrl} + 2m^2_{\widetilde{\ell}_R}E_{maxrl} + 2m^2_{\widetilde{\chi}_1^0}E_{maxrl} - 2E_{cm}m^2_{\widetilde{\chi}_1^0}) + \\
&\qquad 2m^2_{\widetilde{\chi}_1^0}E^2_{cm}E_{maxrl} - 2m^2_{\widetilde{\ell}_R}m^2_{\widetilde{\chi}_1^0}E_{maxrl} + E_{cm}m^4_{\widetilde{\chi}_1^0} = 0
\end{aligned}$$

Tables 7 and 8 show the masses of the $\widetilde{\chi}_1^0$, the $\widetilde{\ell}_R$, and the $\widetilde{\ell}_L$ for each set of cuts performed.

Table 7: Masses of Supersymmetric particles (in GeV) calculated using end-point energies for standard cuts in addition to the p$_t$ $>$ 40 cut. E_{minrr} = 8.993 GeV, E_{maxrr} = 73.44 GeV and E_{maxrl} = 153.3 GeV. (80% right incident electron polarization.)

Particle	Known Mass	Calculated Mass	Discrepancy
$\widetilde{\chi}_1^0$	128.702	127.618	0.84 %
$\widetilde{\ell}_R$	156.952	155.879	0.68 %
$\widetilde{\ell}_L$	238.213	234.985	1.36 %

Table 8: Masses of Supersymmetric particles (in GeV) calculated using end-point energies for standard cuts in addition to the p$_t$ $>$ 15 cut and cut of events with any electrons between 40 - 100 mrad. E_{minrr} = 9.005 GeV, E_{maxrr} = 73.33 GeV and E_{maxrl} = 153.4 GeV. (80% right incident electron polarization.)

Particle	Known Mass	Calculated Mass	Discrepancy
$\widetilde{\chi}_1^0$	128.702	127.797	0.70 %
$\widetilde{\ell}_R$	156.952	156.052	0.57 %
$\widetilde{\ell}_L$	238.213	235.688	1.06 %

7 60% polarization

If the NLC can't polarize incident electrons by as much as 80%, all is not lost. We ran our simulations with 60% polarized incident electrons and the results were also good.

Figure 15 shows the energy distributions of electrons and positrons that come from each of the four different selectron production modes. Figure 16 is the sum of these plots.

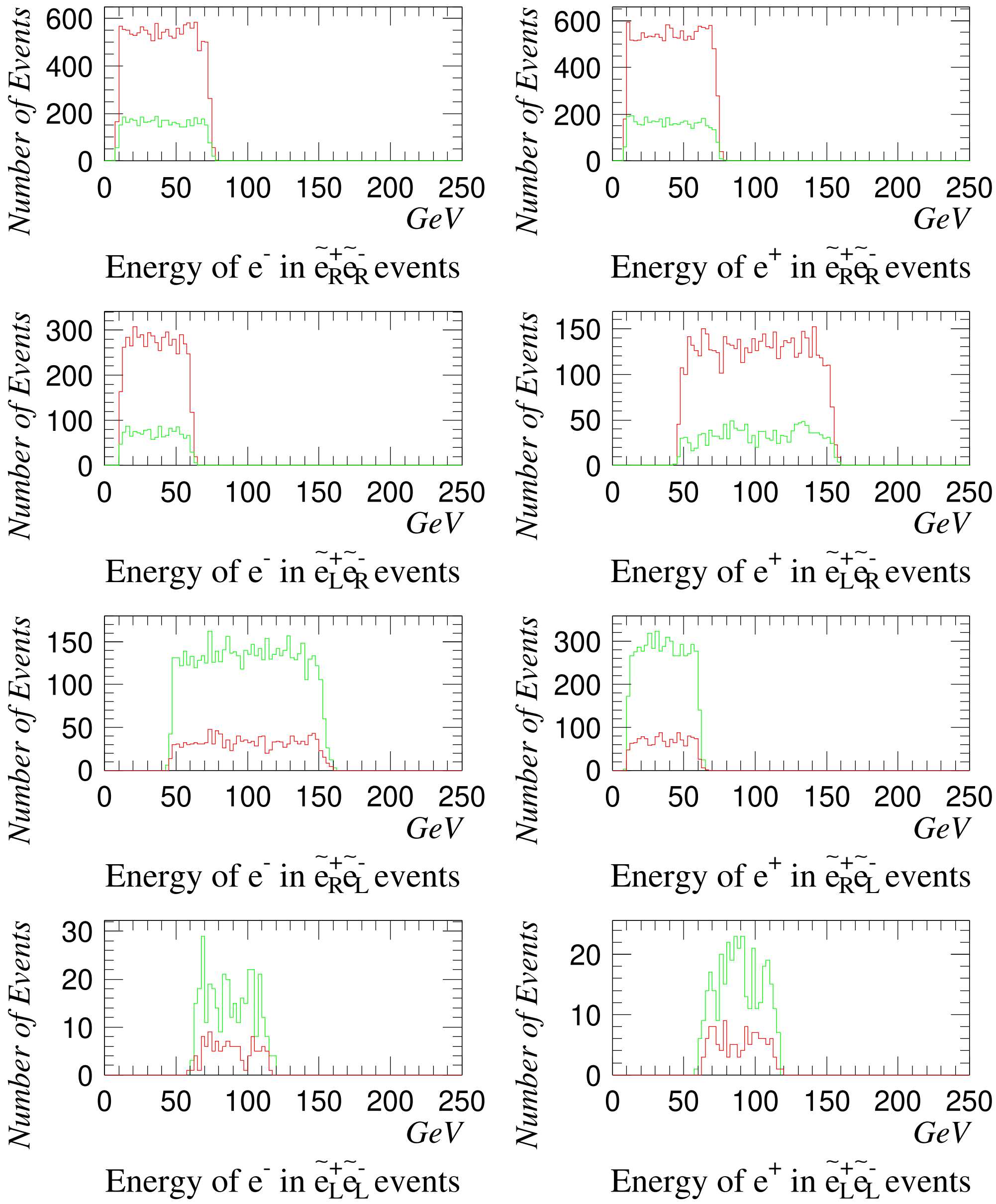

Figure 15: The energy distribution of electrons and positrons that come from the various selectron production modes. The 60% right polarized data is red, the 60% left polarized data is green. This data represents 50 fb^{-1} of data.

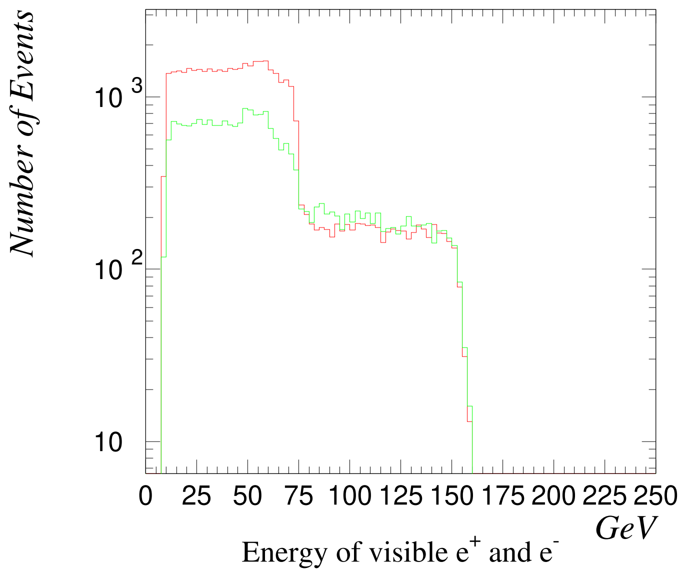

Figure 16: The energy distribution of electrons and positrons that come from selectron events. This is the sum of all the plots in Figure 15. The 60% right polarized data is red while the 60% left polarized data is green. This data represents 50 fb^{-1} of data.

Cut 1 Figure 17 shows the Standard Model background (blue) and Supersymmetric signal (red) at 500 GeV, 60% right polarization, after limiting the events to those with exactly two visible particles: one electron and one positron.

Cut 2 The second cut, Figure 18, limits the events to those that have less than 1 GeV visible energy between $.90 < |\cos(\theta)| < .995$.

Cut 3 Figure 19 only includes events with visible energy in the forward direction less than 1/2 E_{cm} minus 10% E_{cm}.

Figure 20 shows the total p_t for selectron events and for two photon events.

Figure 21 shows the energy distribution of electrons and positrons in both selectron and $\gamma^*\gamma^*$ events as the p_t cut is varied. When the total p_t cut is set at 40 GeV/c, most of the $\gamma^*\gamma^*$ background is removed.

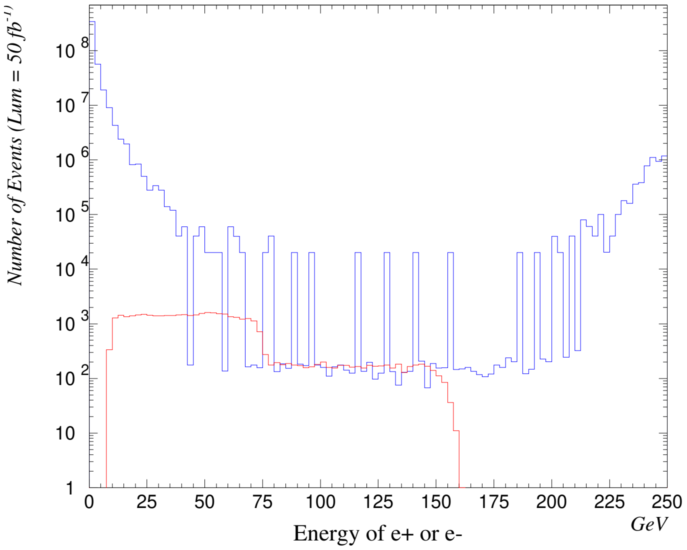

Figure 17: E_{e^+,e^-} for Supersymmetric signal (red) and Standard Model background (blue) following cut to limit events to those with exactly two visible particles: one electron and one positron. E_{cm} = 500 GeV, 60% right polarization.

Figure 22 shows all the Standard Model backgrounds along with the selectron signal when the three standard cuts are made in addition to a p_t cut of 40 GeV/c.

Figure 23 shows the energy distribution of all visible electrons and positrons in both selectron and Standard Model events after all five cuts are applied:

- The three standard cuts described above
- The total p_t must be greater than 15 GeV/c
- Cut events with electrons with an angle between 40 mrad and 100 mrad. This cut amounts to assuming that the detector can see down to 40 mrad.

Most of the background is removed with these cuts, and the signal's endpoints and relative heights remain almost unaffected.

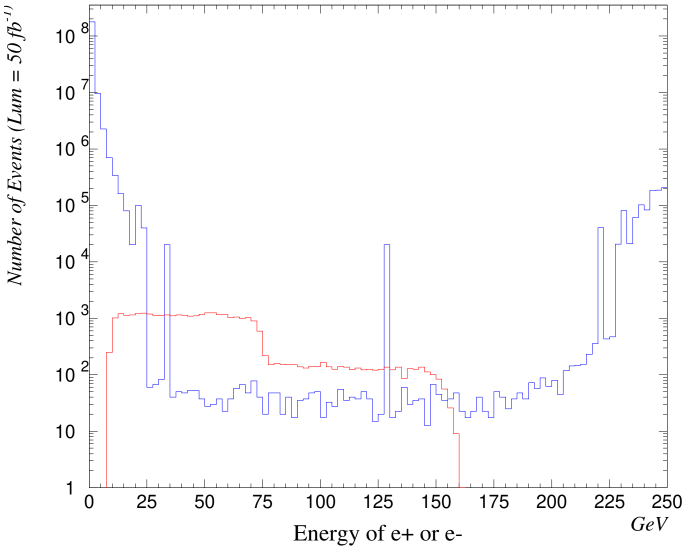

Figure 18: E_{e^+,e^-} for Supersymmetric signal and Standard Model background following cut to limit events to those with less than 1 GeV visible energy between 0.9< $|\cos(\theta)|$ <.995. E_{cm} = 500 GeV, 60% right polarization.

7.1 Mass Calculation for 60% polarized data

For the 60% polarized incident electron data, E_{minrr} = 9.1076 GeV, E_{maxrr} = 73.095 GeV and E_{maxrl} = 153.46 GeV.

Tables 9 and 10 show the masses of the $\widetilde{\chi}_1^0$, the $\widetilde{\ell}_R$, and the $\widetilde{\ell}_L$.

Table 9: Masses of Supersymmetric particles (in GeV) calculated using end-point energies for 60% polarized incident electrons for standard cuts and p_t > 40. E_{minrr} = 9.106 GeV, E_{maxrr} = 73.09 GeV and E_{maxrl} = 153.4 GeV. (60% right incident electron polarization.)

Particle	Known Mass	Calculated Mass	Discrepancy
$\widetilde{\chi}_1^0$	128.702	128.571	0.10 %
$\widetilde{\ell}_R$	156.952	156.932	0.013%
$\widetilde{\ell}_L$	238.213	237.940	0.12 %

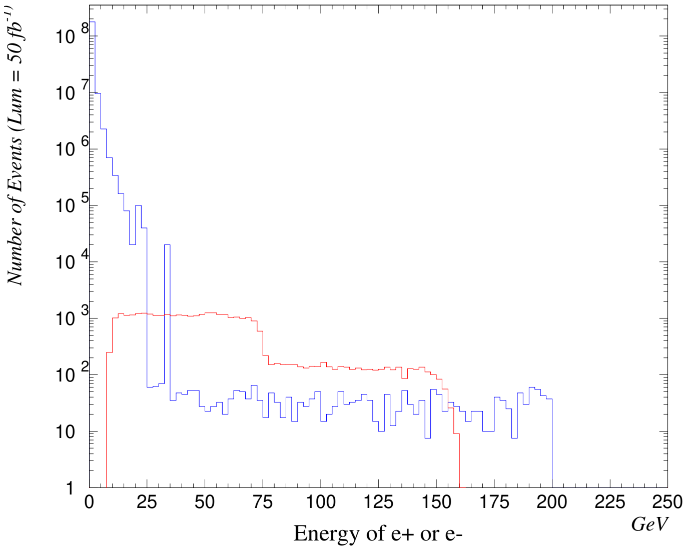

Figure 19: E_{e^+,e^-} for Supersymmetric signal (red) and Standard Model background (blue) following cut to limit events to those with energy in the forward direction less than 0.4 E_{cm}. E_{cm} = 500 GeV, 60% right polarization.

Table 10: Masses of Supersymmetric particles (in GeV) calculated using endpoint energies for 60% polarized incident electrons for standard cuts and $p_t > 15$ cut and cut of events with any electrons between 40 - 100 mrad. E_{minrr} = 9.043 GeV, E_{maxrr} = 73.23 GeV and E_{maxrl} = 153.6 GeV. (60% right incident electron polarization.)

Particle	Known Mass	Calculated Mass	Discrepancy
$\widetilde{\chi}_1^0$	128.702	128.099	0.47 %
$\widetilde{\ell}_R$	156.952	156.392	0.36 %
$\widetilde{\ell}_L$	238.213	236.989	0.51 %

8 Conclusion

We have simulated the expected number of e^+e^- events at a luminosity of 50 fb^-1 per year. We simulated 500 GeV events with 80% and 60% left and

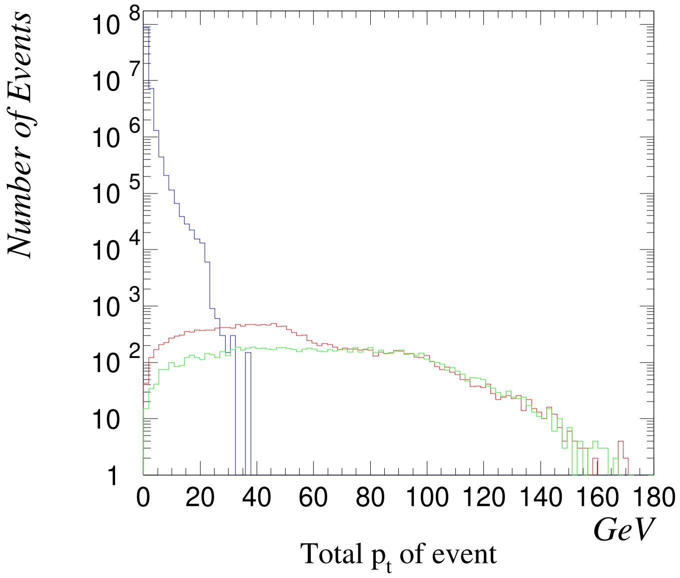

Figure 20: The total transverse momentum of $\gamma^*\gamma^*$ events (blue) and selectron events (red for 60% right polarized data, green for 60% left polarized data). This represents 50 fb^{-1} of data.

80% and 60% right incident electron polarization. With the exception of the $\gamma^*\gamma^*$ background, we have isolated the signal from Supersymmetric selectrons using cuts that are reproduceable in a particle detector. These cuts are:

1. There must be exactly two visible particles: one electron and one positron.
2. There must be less than 1 GeV of energy in the region $.90 < |\cos\theta| < .995$.
3. There is less than 40% of the center of mass energy in the forward hemisphere.

The cuts for removing the $\gamma^*\gamma^*$ background depend on the capabilities of the detector being used. If the particle detector can see down to only 100 mrad, it can detect the selectron signal and remove most of the $\gamma^*\gamma^*$ background with the additional cut:

4. The total p_t of the event must be greater than 40 GeV/c.

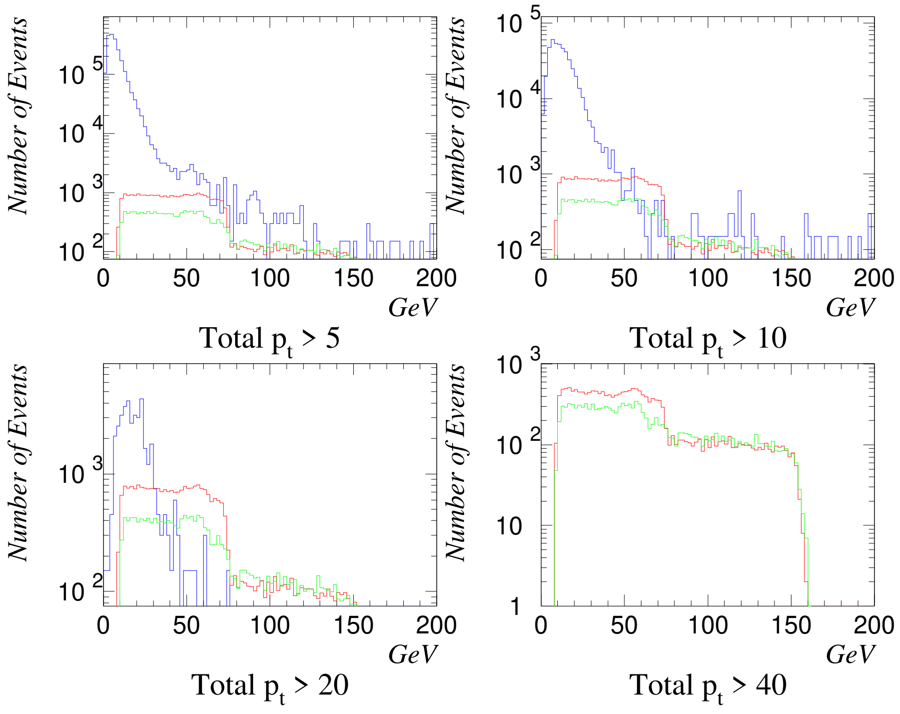

Figure 21: The energy of electrons and positrons as the cut on total transverse momentum is varied. The 60% right polarized selectron data is red, the 60% left polarized data is green, and the $\gamma^*\gamma^*$ data is blue. This represents 50 fb^{-1} of data.

This series of cuts leaves the energy endpoints unchanged, allowing a calculation of the mass of the $\tilde{\chi}_1^0$and $\tilde{e}^{\pm}$, but the relative heights of the boxes are affected. This makes a determination of the cross sections difficult. However, if the detector can see down to 40 mrad, the first three cuts above can be used and the fourth can be replaced by the following two.

4. The total p_t must be greater than 15 GeV/c

5. Cut events with electrons that with an angle between 40 mrad and 100 mrad. This cut amounts to assuming that the detector can see down to 40 mrad.

This series of cuts leaves the energy endpoints and the relative heights of the signal nearly unchanged, allowing for the mass calculation as well as the

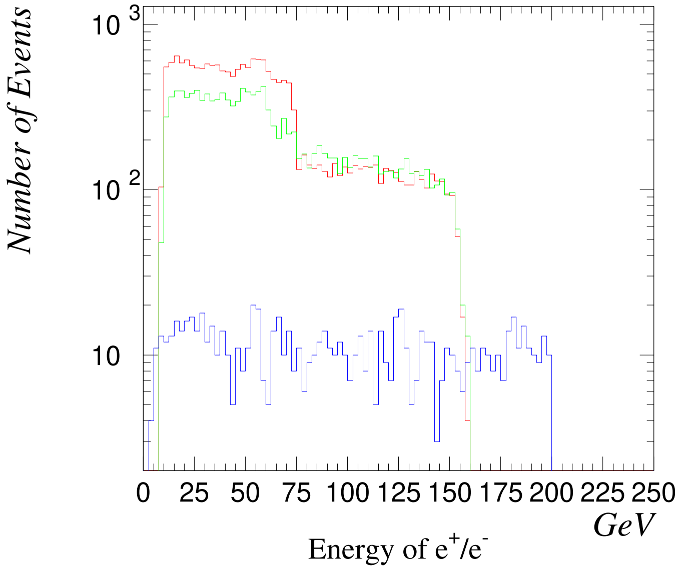

Figure 22: The energy of electrons and positrons in Standard Model (blue) and selectron events (red for 60% right, green for 60% left) with the three standard cuts and a p_t cut of 40 GeV/c.

relative branching ratio determination.

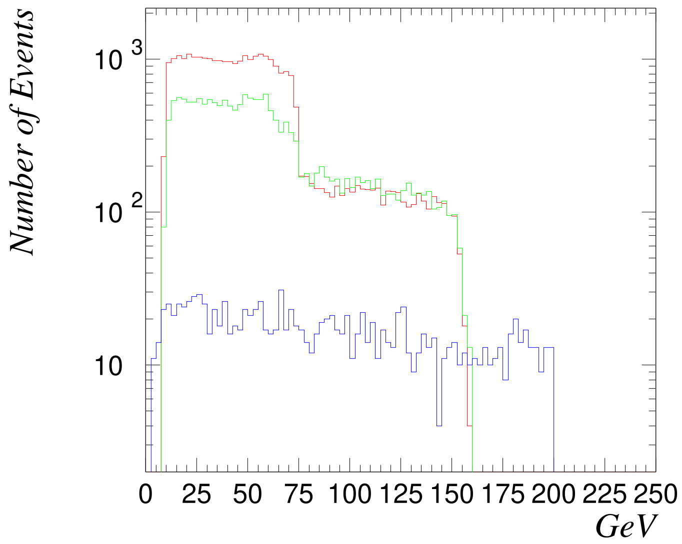

Figure 23: The energy of electrons and positrons after the five cuts described in the paper. Red is 60% right polarized selectron events, green is 60% left polarized selectron events, and blue is Standard Model events. This represents 50 fb^{-1} of data.

References

[1] S. Kuhlman *et al.*, *Physics and Technology of the Next Linear Collider*, BNL 52-502, Fermilab-PUB-96-112, LBNL-PUB-5425, SLAC Report 485, UCRL-ID-124160, submitted to the Snowmass '96 conference, p. 61. 1996.

[2] H. Baer *et. al.*, "Determination of Supersymmetric Particle Cross Sections and Angular Distributions at a High Energy Linear Collider." in appendix of *Physics and Technology of the Next Linear Collider*, BNL 52-502, Fermilab-PUB-96-112, LBNL-PUB-5425, SLAC Report 485, UCRL-ID-124160, submitted to the Snowmass '96 conference, 1996.

[3] F. Paige, S. Protopopescu, in *Supercollider Physics*, p. 41, edited by D. Soper (World Scientific, 1986); H. Baer, F. Paige, S. Protopopescu, and X. Tata in *Proceedings of the Workshop on Physics at Current Accelerators and Supercolliders*, edited by J. Hewett, A. White, and D. Zeppenfeld (Argonne National Laboratory, 1993).

[4] Danielson, N. "Determining the Mass of the Sneutrino and the Chargino by Examining the Sneutrino Sneutrino Production Mode." COLO HEP 404. May, 1998, http://hep-www.colorado.edu/SUSY/.

[5] Goodman, E. "The Search for the Supersymmetric Selectron." COLO HEP 398. April, 1998, http://hep-www.colorado.edu/SUSY/.

[6] Williams, B. "Study of the Production of Supersymmetric Particles." COLO HEP 402. May, 1998, http://hep-www.colorado.edu/SUSY/.

[7] Marchesini, G., Webber, B. R., Abbiendi G., Knowles I. G., Seymour M. H., and Stanco L. "HERWIG." *Computer Phys. Commun.* **67**, 465, 1992.

[8] Schulte, D. in Appendix A of "Study of Electromagnetic and Hadronic Background in the interaction region of the TESLA Collider." University of Hamburg, unpublished. 1996, http://www.slac.stanford.edu/ twmark/nlc/GUINEA_PIG/.